Methyl tunnelling and rotational potentials in solid xylenes and fluorotoluenes

1990 J. Phys.: Condens. Matter 2 8625

(http://iopscience.iop.org/0953-8984/2/43/008)

J. Phys.: Condens. Matter 2 (1990) 8625–8638. Printed in the UK

Methyl tunnelling and rotational potentials in solid xylenes and fluorotoluenes

M Prager†, R Hempelmann†, H Langen‡ and W Müller-Warmuth‡

† Institut für Festkörperforschung des Forschungszentrums Jülich, Postfach 1913, D-5170 Jülich, Federal Republic of Germany

‡ Institut für Physikalische Chemie der Westfälischen Wilhelms-Universität Münster, Schlossplatz 4/7, D-4400 Münster, Federal Republic of Germany

Received 8 March 1990, in final form 11 June 1990

Abstract. CH_3 rotational excitations have been investigated in solid xylenes and fluorotoluenes using inelastic neutron scattering (INS) and nuclear magnetic resonance (NMR) techniques. For two of the six materials the temperature dependence of the tunnel line (shift and broadening) has been compared with the density of states and the slopes of the NMR-T_1 data. The rotational potentials have been derived from tunnel splittings, librational excitations and activation energies. The tunnel energies have been found to occur between 0.026 and 26 μeV. In one case non-equivalent methyl groups have been identified. As compared with results from isolated molecules the potentials of ortho isomers are distinguished by a considerable intramolecular contribution, while the rotational potential of the para and meta compounds are governed by intermolecular interactions. The hindering potential calculated for p-xylene on the basis of pair potentials is inconsistent with the experimental results; reasons will be discussed.

1. Introduction

Methyl rotation of CH_3-substituted benzenes and benzene derivatives has already been the subject of several studies both in the gaseous phase [1–7] and in the solid state [8–18]. Microwave and fluorescence spectra of the isolated molecules showed the effect of substituting a second ring hydrogen by a halide atom or by another methyl group. For fluorotoluenes it was found that only fluorine atoms in the ortho position, i.e. in the immediate neighbourhood of the methyl group, produce strong rotational potentials of dominantly threefold symmetry [6]. The rotational potentials are, however, almost vanishing for the m- and p-isomers [1, 2, 6]. For symmetry reasons the remaining local potential then has important sixfold contributions, particularly in the p-compounds. The xylenes show the same type of systematic changes. The potential barrier for o-xylene is available in the ground and excited electronic states [4]; the rotation is hindered by a rather strong threefold potential. The methyl rotational potentials of the meta and para compounds are of sixfold symmetry and very weak [7].

If the intramolecular contribution to the rotational potential of the methyl group is known for the isolated molecules, it is interesting to determine the additional intermolecular interactions in the solid state. Indeed there exist some nuclear magnetic resonance studies of such systems, and NMR-T_1 measurements of methyl benzenes were even the first experiments of all to demonstrate the influence of rotational tunnelling [8–

0953-8984/90/438625 + 14 $03.50

10]. It was found that the potential barriers hindering the methyl group rotation are still weak in the solid, but large in comparison with the free molecules. At that time information was incomplete, however, and the theory was not yet sufficiently developed to obtain all the details of the methyl rotation and the potentials.

Since then more sophisticated techniques, such as inelastic neutron scattering, especially high resolution tunnelling spectroscopy, have been shown [19–22] to yield much more direct and accurate information on methyl rotational potentials. NMR methods, in addition, profit from a better theoretical understanding of spin–lattice relaxation (T_1) data [23, 24] and from the development of field-cycling level-crossing spectroscopy [25, 26]. Tunnel splittings above about 0.5 μeV can be measured by INS, and those below this value by NMR level-crossing. The potentials can be derived immediately from the tunnelling frequency, librational excitation (measured by INS) and activation energy (NMR). We apply these techniques to xylene and fluorotoluene isomers, and earlier results will be included in the discussion.

A special appeal of such investigations consists of a comparison of intra- and intermolecular interactions, and if the rotational potential is of either type only, a deeper understanding of its origin may be obtained. In particular, if the crystal structure is known, as for p-xylene [27] where the interaction is intermolecular, it should be possible to calculate the rotational potential from pair potentials. So far there is only one system, solid nitromethane [28], which has been studied in this respect. Compared with nitromethane, p-xylene consists of hydrogen and carbon atoms only, where the pair potentials between these two elements are especially well established [29]. Since there are fewer different types of atoms in the molecule, the number of parameters is considerably reduced.

2. Experimental procedure

All materials were purchased from Merck and had a chemical purity >99%. They were used without further purification. From the NMR samples, before sealing the glass ampoules, oxygen was removed by several freeze–pump–thaw cycles. 2- and 4-fluorotoluene may remain in a glassy state after solidification. They need appropriate heat treatment to become crystalline. They had to be cooled down to about 100 K, then warmed to a temperature just below the melting point, and then annealed for some time at this temperature.

Neutron scattering experiments were performed at the IN10 backscattering and IN5 time of flight instruments of the Institut Laue Langevin, Grenoble, and the backscattering spectrometer and the thermal time of flight spectrometer SV22 of the KFA Jülich. The backscattering spectrometer in Jülich was used in two ways: in the normal configuration with a Si monochromator the energy window comprises $-15\ \mu\text{eV} \leqslant \hbar\omega \leqslant +15\ \mu\text{eV}$, whereas in the offset configuration with a $Si_{0.5}Ge_{0.1}$ monochromator the energy range $-2\ \mu\text{eV} \leqslant \hbar\omega \leqslant +32\ \mu\text{eV}$ is covered. The high resolution tunnelling spectra were recorded at sample temperatures around $T_s = 5$ K. The energy resolution was adjusted between 0.4 and 20 μeV. The energy range of librational and lattice modes was usually recorded at two different temperatures. The temperature dependence of the van Hove singularities in the density of states allows a rough estimate of how to assign the corresponding modes [30]. Here the energy resolution was usually $\delta E = 1.8$ meV.

The spin–lattice relaxtion time T_1 was measured in the same way as described in previous papers [24, 31, 32]. 90°–τ–90° pulse sequences were applied at ^{1}H NMR

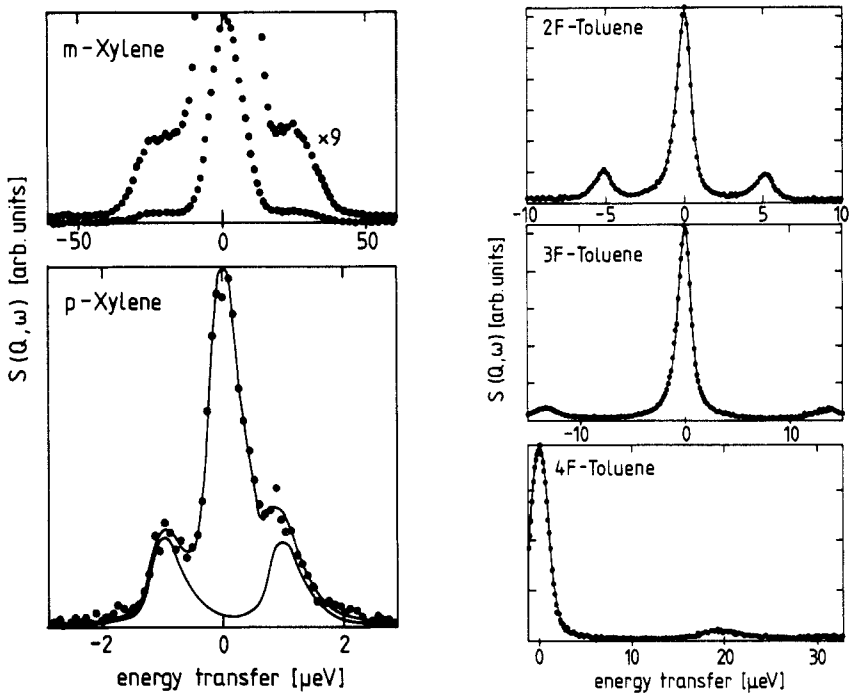

Figure 1. Tunnelling spectra as measured with various high resolution neutron spectrometers. m-xylene, IN5 (ILL); $Q = 1.0$ Å^{-1}; $\delta E = 15$ μeV, $T = 4.5$ K. p-xylene, IN10 (ILL); $Q = 1.85$ Å^{-1}; $\delta E = 0.4$ μeV, $T = 4.5$ K. 2F-toluene, backscattering (KFA); $Q = 1.80$ Å^{-1}; $\delta E = 1$ μeV, $T = 5$ K. 3F-toluene, backscattering (KFA), $Q = 1.85$ Å^{-1}; $\delta E = 1$ μeV, $T = 15$ K. 4F-toluene, backscattering (KFA), $Q = 1.62$ Å^{-1}; $\delta E = 2$ μeV, $T = 5$ K.

frequencies of $\omega_0/2\pi = 15$ and 30 MHz, and T_1 was obtained from the initial slope of the plot $\ln[(M_0 - M_z)/M_0]$ against time (the components of the proton magnetization have the usual meaning). The accuracy of the $1/T_1$ data suffers from the non-exponentiality of the relaxation in some temperature regions and is of the order of $\pm 10\%$. Since the symmetry-restricted spin diffusion model [33] was not yet known and the non-exponentiality ignored when the first measurements on xylenes and fluorotoluenes were carried out [8, 9], all the materials were now re-examined. Level-crossing spectroscopy was applied to measure the tunnelling frequencies of o-xylene. As in previous papers [24, 31] we used a home-made and fully automated field-cycling spectrometer to record the relaxation peaks that occur when the Zeeman and tunnel splittings match.

3. Results and data evaluation

Inelastic neutron scattering spectra obtained for five of the investigated materials in the μeV range are shown in figure 1. The full curves represent fits with a set of resolution functions, one for the elastic line and a shifted one for each tunnelling transition. A constant background is taken into account. The results of the fits are represented in table 1 and include the line positions $\hbar\omega_t^0$ and relative intensities R. For 4F-toluene and 3F-toluene the temperature dependence of the tunnel line was investigated. Spectra of 4F-toluene are represented in figure 2 for seven different temperatures. The convolution fitting procedure yields the position and width of the tunnelling line at the indicated

Table 1. Tunnel splittings $\hbar\omega_t^0$ and their relative intensities $R_{exp} = I_{inel}/I_{el}$ as derived from the spectra of figure 1. The relative intensities R_{CH_3} for an isolated methyl group and R_{th} for a methyl group attached to the xylene or fluorotoluene ring were calculated for the respective momentum transfers Q. The activation energies E_a^S and E_a^Γ describe the temperature dependence of the shift and broadening of the tunnel lines (figure 3).

	Xylenes			Fluorotoluenes		
	Ortho-	Meta-	Para-	Ortho-	Meta-	Para-
$\hbar\omega_t^0$ (μeV)	≤ 0.2	25.6	0.97	5.8	13.8	17.6
R_{exp}	—	0.05	0.25	0.06	0.13	0.04
Q (Å^{-1})	—	−1.0	1.85	1.8	1.85	0.8
R_{CH_3}	—	0.125	0.44	0.40	0.44	0.08
R_{th}	—	0.076	0.21	0.13	0.13	0.035
Occ. rat.		1	1	−0.5	1	1
E_a^S (meV)					7.3	5.5 10.0
E_a^Γ (meV)					10.0	12.5

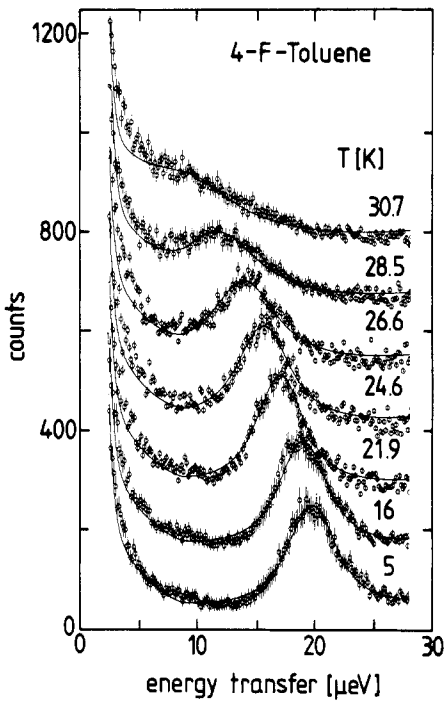

Figure 2. Tunnelling spectra of 4F-toluene taken as the indicated sample temperatures with the backscattering spectrometer of the KFA Jülich in an offset configuration using a $(Si)_{0.9}(Ge)_{0.1}$ mixed crystal as monochromator. Energy resolution $\delta E = 2$ μeV FWHM. The full curves are fits convoluting the scattering function consisting of three Lorentzians at energy transfer $\pm\hbar\omega_t$ and 0 with the measured resolution. The elastic line has ~5800 counts in the maximum.

temperatures (table 2). A fit of the temperature dependence of the line shift by an Arrhenius law (figure 3) yields two temperature ranges $T < 24$ K and $T > 24$ K with activation energies E^S shown in table 1. To describe the line broadening in a similar way an inhomogeneous linewidth of $\Gamma_0 = 1.1$ μeV present at the lowest temperatures was included. Under this assumption we obtain the activation energy E^Γ given in table 1.

An analogous analysis of the results from 3F-toluene (table 3) yields the activation energies represented in table 1. In this case an inhomogeneous line broadening of 0.8 μeV was found. Due to the presence of this inhomogeneous linewidth and some

Table 2. Temperature dependence of the position and width of the tunnelling line in 4 F-toluene as extracted from the spectra of figure 2.

T (K)	$\hbar\omega_t$ (μeV)	Γ (μeV)
5	17.62	1.70
16	16.86	1.62
18.5	16.13	1.31
21.9	15.12	1.54
24.6	13.85	1.85
26.6	12.38	2.40
28.5	10.29	3.16
30.7	8.00	3.80

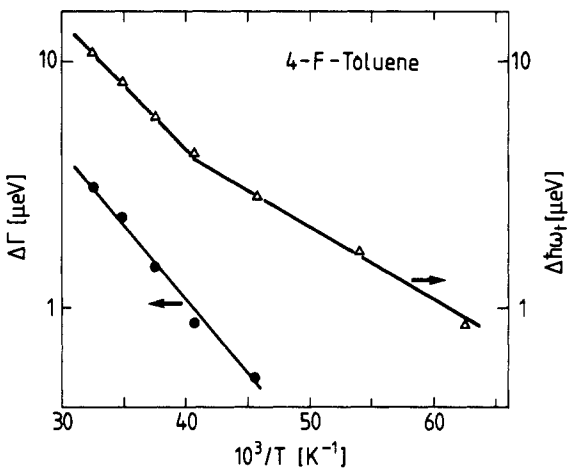

Figure 3. Arrhenius plot of the shift $\Delta\hbar\omega_t$ and broadening $\Delta\Gamma$ of the tunnelling line in 4F-toluene. The derived activation energies are shown in table 1.

Table 3. Temperature dependence of the tunnelling line position and width in 3F-toluene. The values are obtained from spectra taken at the backscattering spectrometer at the KFA, Jülich, $\delta E = 1$ μeV.

T (K)	$\hbar\omega_t$ (μeV)	Γ (μeV)
15	13.48	0.76
20	12.72	0.88
23	11.84	1.05
26	10.88	1.36
29	9.57	1.96

arbitrariness in their determination, the activation energies E_a^Γ are affected by a large error for both materials.

Figure 4 shows a NMR field-cycling scan for o-xylene. The procedure to obtain this spectrum was the same as that described in [31], except that we worked at a smaller starting field B_0 (corresponding to a NMR frequency of 7.6 MHz). The peaks of figure 4 were reproduced several times; they are assigned to the condition $\omega_t^0 = \omega_0$ for the ground state tunnelling frequency. The resulting values for the tunnel splittings are $\omega_t^0/2\pi = 6.4$ MHz and 8.9 MHz.

Inelastic neutron spectra taken with an energy resolution around 1 meV reveal the lattice vibrations and the methyl librations (figure 5). In most cases spectra were also

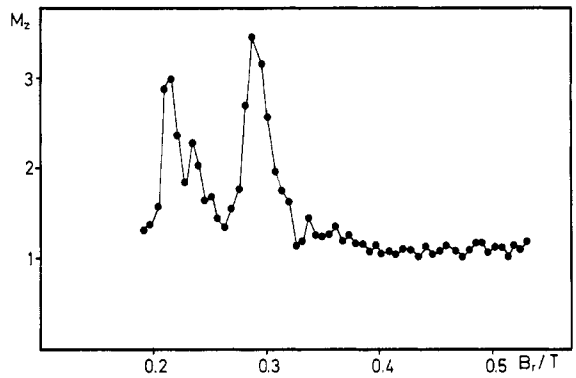

Figure 4. NMR field-cycling spectrum of o-xylene. The M_z component of the proton magnetization in arbitrary units is plotted against the magnetic reference field B_r which was varied in steps of 0.01 T.

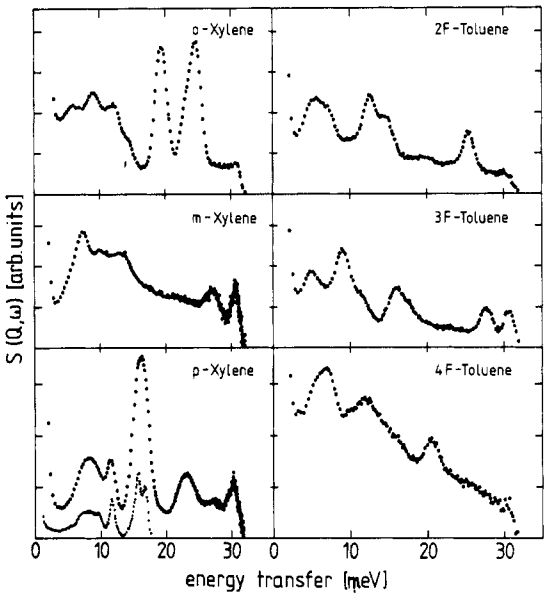

Figure 5. INS spectra of the xylenes and fluorotoluenes as measured with the time of flight spectrometer SV 22 at the FRJ2 at the KFA, Jülich. Standard programs were used to transform the data to $S(\Theta, \omega)$. The incident wavelength was $\lambda_i = 1.5$ Å, and the energy resolution at the elastic line $\delta E = 1.8$ meV. The sample temperature was $T = 18$ K. A measurement with improved energy resolution ($\delta E = 1$ meV) shows that the strongest line in p-xylene is a doublet.

measured at increased sample temperatures (not shown). The peak positions in these spectra are given in table 4. Some of the values are taken from other spectra recorded with different energy resolution or in another energy range. The damping of a strong peak with increasing sample temperature [30] and/or the value of the low-temperature slope of the NMR-T_1 curve are used to assign the librational modes. In table 4 peaks identified in this way as librations are labelled with an 'L' following the number. The librational peaks of m-xylene and 4F-toluene are comparatively small, and their assignment is less clear than that of the other materials. No special attempt was made to identify higher excited librational modes.

Spin–lattice relaxation rates of m-xylene, 2F-toluene and 3F-toluene are more or less in agreement with those previously measured [8, 9]. p-xylene was recently re-examined [24]. The results for o-xylene and 4F-toluene are shown in figure 6. The full curves correspond to curve fittings based on Haupt's equation [23]

Table 4. Peak positions in the density of states of the xylenes and fluorotoluenes as extracted from figure 5. All values are in meV. Some of the values were obtained from similar measurements performed in different energy ranges with different resolution. The identified methyl librational modes are labelled by L.

Xylenes			Fluorotoluenes		
Ortho-	Meta-	Para-	Ortho-	Meta-	Para-
4.7			5.0		
5.9			6.3	5.0	5.7
6.6	7.05	7.3	7.6	7.9	7.00
8.6		9.7		9.1L	
10.6	9.9L	11.8		11.4	
12.2			12.78		12.60L
14.4	13.24	15.9L	14.7L	16.2	
19.0L		16.9L			20.53
23.0L		23.0			
24.3	26.8	27.2	25.6	27.8	
	30.4	30.2		30.7	
34.7	34.7				
39.2				37.0	39.1
41.7				42.3	43.5
51.0	50.3			45.9	
55.4	54.5			55.5	52.3

$$1/T_1 = C_1 \sum_{n=-2}^{+2} \frac{n^2\tau_c}{1+(\omega_t + n\omega_0)^2\tau_c^2} + C_2 \sum_{n=1}^{2} \frac{n^2\tau_c}{1+n^2\omega_0^2\tau_c^2} \tag{1}$$

The relaxation strength C_1 accounts for dipole–dipole interactions which are connected with a change of symmetry of the CH_3 rotor from A to E. C_2 takes notice of transitions without change of symmetry, which are forbidden if only intramethyl couplings are considered.

The temperature dependence of the correlation time τ_c and the tunnelling frequency ω_t were again approximated by [24]

$$\tau_c^{-1} = (\tau_0')^{-1} \exp(-E_A'/RT) + (\tau_0'')^{-1} \exp(-E_A''/RT) \tag{2}$$

and

$$\omega_t = \frac{\omega_t^0}{1+aT^6}.$$

The limiting value E_A' may be identified with the activation energy E_A for CH_3 reorientation. E_A'' was previously found to approach E_{01}, the energy separation between the librational ground and first excited states if the barrier E_A is below about 4 kJ mol^{-1}. The coefficient a is characteristic of the respective system and amounts to 10^{-11}–10^{-10} K^{-6}. New curve fits were made for the $1/T_1$ data of all six materials. $1/T_1$ of o-xylene could only be described by the superposition of two curves of the type of equation (1) with (2). The various parameters are listed in table 5.

4. Discussion

4.1. Equivalence of methyl groups

For p-xylene we know from the crystal structure that all methyl groups are equivalent. This agrees with the result of our experiments. For o-xylene the two tunnel transitions

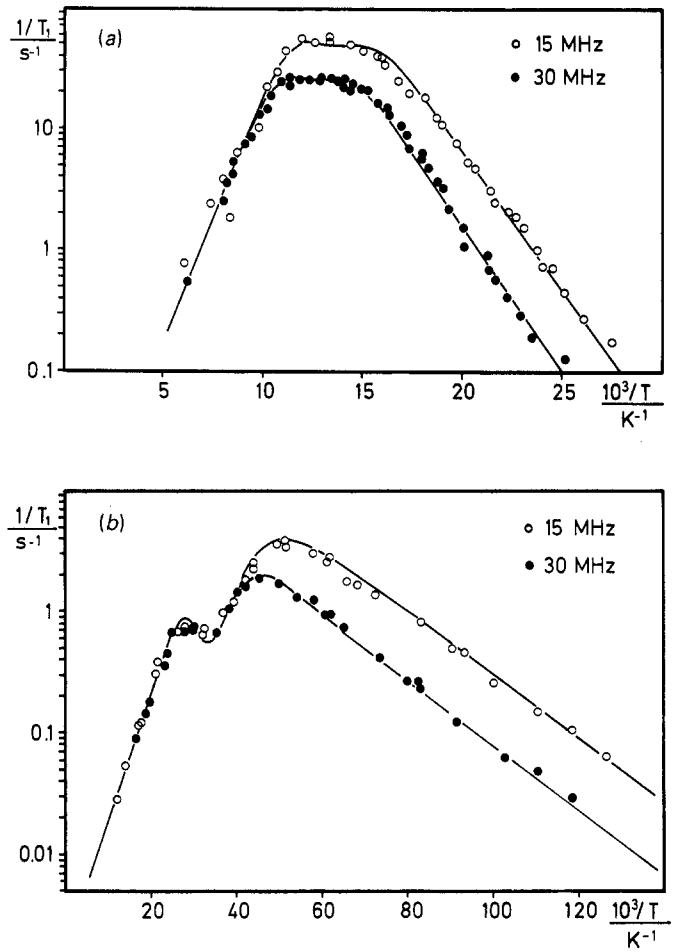

Figure 6. Experimental proton spin–lattice relaxation rates (points) for (*a*) o-xylene and (*b*) 4F-toluene plotted against reciprocal temperature. The full curves correspond to the best fit using the procedure outlined in the text and the parameters of table 3.

Table 5. Numerical parameters as derived from the T_1 measurements and fitting procedures. The details are given in the text.

	E_A (kJ mol^{-1})	τ'_{co} (10^{-13} s)	C_1 (10^9 s^{-2})	τ''_{co} (10^{-10} s)	E''_A (kJ mol^{-1})	C_2 (10^9 s^{-2})
0-xylene	7.1	0.5	1.0	0.03	4.4	1.0
	8.0	1.0	1.1	0.04	6.0	1.2
m-xylene	1.5	9.5	0.48	0.24	0.74	0.50
p-xylene	4.5	1.0	2.1	0.20	3.5	1.3
2F-toluene	2.5	6.0	0.68	7.0	1.1	0.34
3F-toluene	2.2	6.0	0.46	5.0	0.64	0.21
4F-toluene	1.9	1.3	2.2	6.1	0.48	0.31

in the field-cycling spectra (figure 4) and the two librational peaks (figure 5) as well as the $1/T_1$ against $1/T$ plot (figure 6) are indications of the presence of two inequivalent methyl groups. The alternative explanation that a coupling between adjacent CH_3 groups may be responsible for the librational doublet [11], as already observed in other systems [34], can be ruled out in view of the additional experimental data: already the most simple approach for tunnelling of coupled methyl groups [35, 36] shows that the numerical values would be inconsistent.

For the other compounds we can guess from the relative intensity R_{exp} of the tunnel peaks of the neutron spectra the probability of occurrence of the corresponding methyl group [19, 37]. A theoretical intensity ratio R_{CH_3} is calculated for the three protons of the CH_3 groups, averaged for good powders and assuming single phase systems. These calculated values might be different from the observed ratios for various reasons: at first some samples may contain additional atoms which contribute to the elastic scattering. Secondly the samples are obtained from the liquid state and might have preferential orientations. Finally some of them may not be completely crystalline (see introduction).

The dominant parasitic elastic scattering in our samples is given by the presence of protons not contained in the methyl groups. If there are n methyl groups in the molecule and m additional protons we can express the total elastic scattering I^{el}_{tot} as a function of the theoretically expected scattering from a single CH_3 group $I^{el}_{CH_3}$

$$I^{el}_{tot} = nI^{el}_{CH_3} + (m/3)I^{el}_{CH_3}(1 + 2R_{CH_3})$$

where $R_{CH_3} = I^{inel}_{CH_3}/I^{el}_{CH_3}$ is the theoretically [19] expected ratio of tunnelling to elastic intensity of one methyl group at the momentum transfer Q used in the experimental set-up. The experimentally expected ratio $R_{th} = I^{inel}_{CH_3}/I^{el}_{tot}$ then reads

$$R_{th} = R_{CH_3}/[1 + (m/3n)(1 + 2R_{CH_3})]. \tag{3}$$

These numbers are also shown in table 1. Comparing R_{th} with the ratio determined experimentally we can conclude that m- and p-xylene and 3F- and 4F-toluene contain only equivalent methyl groups. In 2F-toluene the measured value R_{exp} would be consistent with the presence of a second type of CH_3 group having the same probability of occurrence as the observed one. We could not control, however, whether parts of this sample were in a glassy state. The librational doublet of 2F-toluene (figure 5) represents a limit of non-equivalent methyl groups.

On the other hand, despite the existence of just one type of methyl group the librational peak in p-xylene is a doublet (figure 5). This can only be explained by a dispersion of the librations or by a direct methyl–methyl interaction. The theoretical approach of coupled methyl groups [35] yields in harmonic approximation a weak interaction potential W_3 from the relation $W_3/V_3 = \Delta E/E = 1/16$. This interpretation is supported by the crystal structure [27] showing that there are two adjacent CH_3 groups.

4.2. Rotational potentials and activation energies

The rotational potential of the methyl group is parametrized as usual by a Fourier expansion including two terms and a phase factor $(-1)^k$

$$V(\varphi) = \sum_{n=1}^{2} \tfrac{1}{2}V_{3n}[1 + (-1)^k \cos 3n\,\varphi]. \tag{4}$$

The eigenvalues of the corresponding Schrödinger equation

$$\left(-B\frac{d^2}{d\varphi^2} + V(\varphi) - E\right)\psi = 0 \tag{5}$$

are tabulated in the relevant range of potential parameters [38].

Using this model we may deduce the rotational potential, equation (4), from the observed parameters $\hbar\omega_t^0$, E_{01}, and E_A (tables 1, 4 and 5). In principle, two solutions are obtained, one with dominating threefold and the other one with dominating sixfold potential. The correlation of a large number of methyl tunnel splittings and activation energies and/or relaxation rate maxima [31] suggests that the solution with $V_3 \gg V_6$ is the correct one. This is in agreement with a compilation of methyl rotational potentials in solids [39]. The V_3 and V_6 results are shown in table 4 together with the measured transition energies. Since the dependence of E_i on V_3 and V_6 in equation (5) is non-linear, the accuracy of the potential values is different from case to case. It is particularly poor for 3F- and 4F-toluene.

For all six solid systems $\hbar\omega_t^0$, E_{01} and E_A are available from the experiments, so that the solutions of equation (5) with (4) are overdetermined. This may be taken as a control that the data really belong to the same solution, which is the case here within the limits of accuracy. The rotational potentials thus obtained are at variance with those previously estimated for some of the compounds [8, 9]. At that time ω_t^0 and E_{01} could not yet be measured and comparison of the NMR-T_1 curves was only made with a few thermodynamic measurements of little accuracy.

Previous studies have shown that E_{01} can also be taken from the low-temperature decay of $1/T_1$ in an Arrhenius plot provided the hindering potential is below about 4 kJ mol^{-1} [24]. Comparison of E''_A and E_{01} data (tables 4 and 5) suggests, however, that this rule is no longer valid for m-xylene, 3F-toluene and especially 4F-toluene. In all these cases (and there are in addition some unpublished data with similar results) the INS spectra contain close to the librational excitation a vibration peak whose energy is not far from the experimental E''_A value. More important, these E''_A values agree with the E^S_A data of table 1 derived from the temperature shift of the tunnelling frequencies of 3F- and 4F-toluene.

In the case of 4F-toluene it was rather unexpected to observe two temperature ranges with different slopes for the shift of the tunnel lines (figure 3). The two activation energies coincide reasonably well with observed densities of states and one—as already stated—with E''_A from the NMR-T_1 experiment.

The activation energies found from the broadening of the tunnelling lines with temperature are very close to the observed librational modes. This behaviour is theoretically predicted and the agreement is rather satisfactory if the experimental errors are kept in mind.

4.3. Comparison with isolated molecules and other methyl benzenes

For the purpose of comparison table 4 also shows the rotational potentials of the isolated molecules. The sytematic behaviour which was observed for the gaseous molecules is no longer present in the solid phases. The ortho compounds have the strongest barrier as in the gas phase. The increase in strength is rather small, however. This means that in the solid state intramolecular forces dominate the hindrance. For meta and para isomers, in contrast, in the solid state the rotational potential is governed by intermolecular forces. The methyl group is no longer hindered by extremely weak potentials of sixfold symmetry as in the free molecules, but by clearly stronger threefold rotational potentials. The barriers for the xylenes are systematically higher than those for the corresponding fluorotoluenes. This may be a result of the additional steric hindrance from other methyl groups.

In spite of the much stronger potentials observed for most of the compounds in the solid state, with the exception of o-xylene, the hindrances remain comparatively small.

Table 6. Rotational potentials (V_3, V_6, k) as derived from the measured tunnel splittings $\hbar\omega_t^0$. Librational energies E_{01} and activation energies E_A. 1 meV = 0.0965 kJ mol^{-1}. For comparison, literature data for the free molecules (gaseous phase) are also listed: [a] ref. [4], [b] ref. [7], [c] ref. [5], [d] ref. [6], [e] ref. [2], [f] ref. [1].

	Experiment			Derived			Isolated molecules	
	$\hbar\omega_t^0$ (μeV)	E_{01} (meV)	E_A (kJ mol^{-1})	V_3 (kJ mol^{-1})	V_6 (kJ mol^{-1})	k	V_3 (kJ mol^{-1})	V_6 (kJ mol^{-1})
o-xylene	0.037	19.0	8.0	8.9	0.9	0	8.4[a]	0
	0.026	23.0	7.1	8.3	0.5	1	6.2[b]	
m-xylene	25.6	9.9	1.5	2.1	0.1	1	0	0.31[b]
p-xylene	0.97	16.0	4.5	4.9	0		0	0.13[b]
2F-toluene	5.8	14.7	2.5	3.1	0.5	1	2.72[c,d]	0.08[d]
3F-toluene	13.8	9.1	2.2	2.9	0.5	0	0.2[d,e]	0.06[d]
								0.09[e]
4F-toluene	17.6	12.6	1.9	2.1	0.7	1	0	0.06[d,f]

This agrees with previous studies of other methyl-substituted benzenes. The most prominent and most intensively studied system is toluene [13, 17, 22]. In the isolated molecule the rotational potential is almost zero [3] and in the solid state it is still weak. However, the presence of two inequivalent rotors in the unit cell [40] makes the data analysis rather complex.

Existing studies of tetra-, penta- and hexamethylbenzene [10, 14–16, 18, 41] and of methyl-ditertiarybutylphenol [42] show that the rotational potentials are relatively weak in general, but increase in the presence of neighbouring methyl groups. Proof of the intramolecular origin due to methyl–methyl coupling was given by the comparison of hexamethylbenzene [14] and 1,3,5-trichloro- 2,4,6-trimethylbenzene [18]. As far as 1,2,4,5-tetramethylbenzene (durene) is concerned, we believe that the multiplet observed in the field-cycling experiment [16] is not due to coupling, but rather to the presence of non-equivalent methyl groups as for o-xylene. A calculation of the tunnel splitting on the basis of a librational state split by the coupling cannot describe the doublet line, but yields a single transition.

The results show consistently that the intermolecular contribution to the rotational potential is weak in all methyl-substituted benzenes. Low barriers are observed in all compounds where a single methyl group is attached to the benzene ring. The potential increases significantly when a second methyl group replaces a proton neighbour. The influence of a neighbouring fluorine atom is less pronounced.

4.4. Rotational potential and pair interaction potentials

For sufficiently strong potentials the methyl libration can be well described in harmonic approximation as lattice modes. The tunnel splitting, on the other hand, depends on the overlap of the wavefunction in adjacent minima of the rotational potential. Thus the anharmonicity influences this value greatly. Pair potentials are widely and successfully used to describe the lattice modes of a crystal. Application of the concept of pair potentials for the rotational excitations of a methyl group will show whether they are also useful if the anharmonic part of the potential becomes important. With pair potentials the lattice dynamics of hydrocarbon systems are based on just six interaction

parameters [29, 43] and the crystal structure. Various sets of parameters were found by different authors.

We are interested in the potential energy at various orientations of one CH_3 group. The principal procedure is straightforward: from the crystal structure one gets all distances R_{ij} from the protons i of the methyl group under investigation to all other atoms of type j and sums all pair interactions. This yields the potential energy for a given orientation φ of the methyl group

$$V(\varphi) = \sum_{ij} \left(\frac{a_{ij}}{R_{ij}^6(\varphi)} - \frac{b_{ij}}{R_{ij}^{n_{ij}}(\varphi)} \right).$$

The parameters a_{ij}, b_{ij} and n_{ij} are taken from [43] and the R_{ij} for p-xylene from [27]. This calculation is performed for different orientations φ of one methyl group. The angular dependent part of $V(\varphi)$ is, apart from a constant basic value, the rotational potential of the methyl group.

Various problems have to be overcome in practice to improve this calculation. At first a methyl group is usually somewhat distorted (bond lengths, bond angles) from the pure C_{3v} symmetry due to the interaction with the surroundings. Thus a rotation by 120° brings the three protons into different positions and yields a different rotational potential strength. In reality, the deformation of the methyl group in the lattice frame after rotation is re-established. We have removed this influence by symmetrizing the methyl group to full C_{3v} symmetry around the rotation axis. This gives the required symmetry of the rotational potential, but may weaken the calculated potential strength somewhat. A calculation performed at this level of approximation yields a rotational potential strength of $VS = 38\ B$ which is considerably lower than calculated from the rotational excitations (table 6).

Another trivial reason for the discrepancy could be the thermal expansion of the lattice. The structure is determined at $T = 180$ K [27], while the inelastic measurements were performed around $T = 10$ K. Oversimplifying the structural changes with T a linear isotropic expansion coefficient of 1.6% can be estimated from the temperature-dependent unit cell volume [27]. A calculation of the rotational potential with the reduced lattice parameters assuming a rigid molecule still yields a too weak potential.

A more important shortcoming is included in the concept of standard structure determinations to describe the density distribution of an atom by a thermal ellipsoid. For motions like librations which are restricted onto the surface of a sphere, this leads to an apparent bond shortening which increases the intermolecular distances and thus diminishes the strength of a calculated rotational potential. Usually a C–H bond length of 1.04 Å is assumed for CH_3 groups. In the structure determination of p-xylene an average bond length of 0.98 Å is extracted, however. Finally, x-rays cannot give sufficiently accurate data on the proton positions.

For all these reasons we may understand why we obtained a potential that was too weak. To perform a reliable calculation of rotational potentials from pair potentials a much more accurate neutron structure determination at $T = 5$ K is required.

5. Conclusions

The methyl rotational potentials of the ortho, meta and para isomers of crystalline xylene and fluorotoluene have been investigated using inelastic neutron scattering in the μeV and meV resolution regime and in addition NMR techniques. The rotational

potentials were found to be weak. Only for the ortho compounds does the (steric) intramolecular hindering lead to somewhat stronger potentials. In the other cases the potential is dominantly created by intermolecular interactions. This is obvious from a comparison with gas phase data. All potentials are predominantly threefold in symmetry. An evaluation of the intensities of tunnel peaks shows further that there exists in general only one type of methyl group in each compound.

An exception is o-xylene where non-equivalent CH_3 groups were detected by NMR field-cycling and T_1 experiments. In the case of p-xylene the conclusion of equivalent CH_3 groups is consistent with the crystal structure, which is not known for the other materials. The rotational potential could be compared with calculations using pair potentials and interatomic distances taken from the structure. While the potential shape is reasonably reproduced its strength is too weak by more than 50%. The comparison was intended to check the validity of pair potentials for distances which determine the barrier height of the rotational potential and thus the tunnel splitting. Considerably improved structural data are needed to achieve progress in this direction.

Acknowledgments

We wish to thank the ILL Grenoble for support and especially Dr H Blank for the help with the experiments on IN5.

References

[1] Rudolph H D and Seiler H 1965 *Z. Naturforsch.* **20a** 1682
[2] Rudolph H D and Trinkhaus A 1968 *Z. Naturforsch.* **23a** 68
[3] Rudolph H D, Dreizler H, Jaeschke A and Wendling P 1970 *Z. Naturforsch.* **22a** 940
[4] Ingham K C and Strickler S J 1970 *J. Chem. Phys.* **53** 4313
[5] Susskind J 1970 *J. Chem. Phys.* **53** 2492
[6] Okuyame K, Mikami N and Ito M 1985 *J. Phys. Chem.* **89** 5617
[7] Breen P J, Warren J A, Bernstein E R and Seemann J I 1987 *J. Am. Chem. Soc.* **109** 3453
[8] Haupt J and Müller-Warmuth W 1968 *Z. Naturforsch.* **23a** 208
[9] Haupt J and Müller-Warmuth W 1969 *Z. Naturforsch.* **24a** 1066
[10] Allen P S and Cowking A 1968 *J. Chem. Phys.* **49** 789
[11] Livingston R C, Grant D M, Pugmire R J, Strong K A and Brugger R M 1973 *J. Chem. Phys.* **58** 1438
[12] Clough S and Heidemann A 1978 *J. Phys. C: Solid State Phys.* **12** 761
[13] Müller-Warmuth W, Schüller R, Prager M and Kollmar A 1979 *J. Magn. Reson.* **34** 83
[14] Takeda S, Soda G and Chihara H 1980 *Solid State Commun.* **36** 445
[15] Clough S, Horsewill A J and Heidemann A 1981 *Chem. Phys. Lett.* **82** 264
[16] Takeda S and Chihara H 1983 *J. Magn. Reson.* **54** 285
[17] Cavagnat D, Magerl A, Vettier C and Clough S 1986 *J. Phys. C: Solid State Phys.* **19** 6665
[18] Takeda S and Chihara H 1987 *Quantum Aspects of Molecular Motions in Solids (Springer Proceedings in Physics 17)* ed A Heidemann *et al* (Berlin: Springer) p 76
[19] Press W 1982 *Single Particle Rotations in Crystals (Springer Tracts in Modern Physics 92)* (Berlin: Springer)
[20] Heidemann A *et al* (eds) 1987 *Quantum Aspects of Molecular Motions in Solids (Springer Proceedings in Physics 17)* (Berlin: Springer)
[21] Prager M and Heidemann A Neutron tunnelling spectroscopy: A compilation of available data *ILL Internal Report* 87PR15T
[22] Cavagnat D 1985 *J. Chim. Phys.* **82** 239 review paper
[23] Haupt J 1971 *Z. Naturforsch.* **26a** 1578
[24] Langen H, Montjoie A-S, Müller-Warmuth W and Stiller H 1987 *Z. Naturforsch.* **42a** 1266 and references therein
[25] van Hecke P and Janssens J 1978 *Phys. Rev.* B **17** 2124

[26] Gabrys B 1984 *Mol. Phys.* **51** 601
[27] van Koningsveld H, van den Berg A J, Jansen J C and de Goede R 1986 *Acta Crystallogr.* B **42** 491
[28] Cavagnat D and Pesquer M 1986 *J. Phys. Chem.* **90** 3289
[29] Williams D E 1967 *J. Chem. Phys.* **47** 4680
Kitaigorodskii A I 1966 *J. Chim. Phys.* **63** 6
[30] Müller-Warmuth W, Schüler R, Prager M and Kollmar A 1978 *J. Chem. Phys.* **69** 2382
[31] Montjoie A-S, Müller-Warmuth W, Stiller H and Stanislawski J 1988 *Z. Naturforsch.* **43a** 35
[32] Müller-Warmuth W, Dupree K H and Prager M 1984 *Z. Naturforsch.* **39a** 66
[33] Emid S and Wind R A 1975 *Chem. Phys. Lett.* **33** 269
[34] Möller K D and Andresen H G 1962 *J. Chem. Phys.* **37** 1800
[35] Häusler W and Hüller A 1985 *Z. Phys.* B **59** 177
[36] Prager M, Heidemann A and Häusler W 1986 *Z. Phys.* B **64** 447
[37] Prager M, Dupree K H and Müller-Warmuth W 1983 *Z. Phys.* B **51** 309
[38] Gloden R F 1970 *Euratom Reports* EUR4349 and EUR4358
[39] Clough S, Heidemann A, Horsewill A J, Lewis J D and Paley M N J 1982 *J. Phys. C: Solid State Phys.* **15** 2495
[40] Anderson M, Bosio L, Bruneaux-Poulle J and Fourme R 1977 *J. Chim. Phys.* **74** 68
[41] Gabrys B and van Gerven L 1981 *Chem. Phys. Lett.* **82** 260
[42] Clough S and Heidemann A 1979 *J. Phys. C: Solid State Phys.* **12** 761
[43] Taddei G, Bonadeo H, Marzocchi M P and Califano S 1973 *J. Chem. Phys.* **58** 966